Monte Carlo calculation of wall correction factors for the air kerma standards of the BEV for ^{137}Cs and ^{60}Co g-rays

Josef Witzani
Bundesamt für Eich- und Vermessungswesen (BEV)
Arltgasse 35
A-1160 Vienna, Austria
e-mail: j.witzani@metrologie.at

Introduction

The standards of air kerma of the BEV for ^{137}Cs and ^{60}Co γ-rays are two cylindrical graphite cavity chambers of the type CC01. They have been compared to the standard of the BIPM in 1994 and 1995 [1, 2]. Up to now the wall correction factors used for these standards are based on the well known extrapolation of the ionisation current measured for different wall thickness. Other authors [3, 4, 5] have pointed out, that wall correction factors determined by this method and by Monte Carlo (MC) calculations are significantly different. Experiments by Büermann et al. [6] have given confidence, that MC calculations lead to correct results, while the extrapolation method cannot provide the proper corrections for the wall effect.

Monte Carlo Calculation

The Monte Carlo code "PENELOPE" (version 2001) [7] was used for the calculation of wall correction factors for the cylindrical graphite cavity chambers, type CC01, SN 125 and SN 132 with a graphite density of 1.72 g/cm³ and 1.80 g/cm³, respectively. A simplified model (see fig. 1) of this chamber with the dimensions given in table 1 was used in the calculations.

The correction factors for attenuation k_{at} and scatter k_{sc} were calculated using an approach described by Rogers and Bielajew [5] and Büermann et al.[6]:

$$k_{at} = \frac{\sum_i E_{i,0} * e^{m_i s_i}}{\sum_i E_{i,0}} \qquad (1)$$

$$k_{sc} = \frac{\sum_i E_{i,0}}{\sum_i (E_{i,0} + E_{i,1})} \qquad (2)$$

In equations (1) and (2) $E_{i,0}$ is the energy, deposited in the cavity of the chamber by electrons, which are generated from the i-th primary photon interaction, μ_l is the linear attenuation coefficient and s_i is the path length of the photon in the wall material to the first interaction point. The energy, deposited by electrons, which are generated by all subsequent interactions contributes to the scatter effect and is taken into account as $E_{i,1}$ in the denominator of equation (2).
The results for the correction factors obtained by the MC - and by the extrapolation technique are given in table 2. The latter technique includes a correction factor k_{cep} for the "centre of electron production" and was applied up to now for the standards of the BEV. This correction is not applicable in the MC technique, since it is implicitly taken into account in the formalism given by the equations (1) and (2). In the MC calculations the type A uncertainty of k_{at} and k_{sc} was 0.01 % and 0.03 %, respectively. The results are in agreement with those from other authors [3,6], who used a different MC-code (EGS4, EGSnrc).

The contribution from the different bodies of the chamber to the primary energy deposited in the cavity was scored and is given in table 3. The small difference between the contribution from the lower and upper wall can be explained by the position of the central electrode. Because the central electrode is directly attached to the lower wall in the MC model, it prevents more electrons from the lower wall from reaching the cavity than from the upper wall. About two third of the energy comes from the cylindrical part of the chamber wall. Furthermore, the angular contribution from the cylindrical wall to the primary energy deposited in the cavity was also scored in the MC calculations. This revealed the expected fact, that the contribution from the front part of the cylindrical wall (facing the radiation source) is much higher than from the rear part (see diagram 1). This effect is present in a parallel as well as in a divergent beam and can be explained by the dominant scatter direction of electrons in the beam direction. But because of the inverse square law the front part of the wall is exposed to a higher photon fluence in a divergent beam, than in a parallel beam. Therefore one could argue, that the effective point of measurement is shifted from the geometrical centre of the chamber towards the source. This effect would lead to an increase of the chamber response, which should be corrected for by a corresponding correction factor less than unity (rough calculations gave a correction factor of 0.994 for the chamber CC01 at 1 m distance corresponding to a shift of the effective point of measurement by about 3 mm towards the source). Boutillon and Niatel [8] took this effect into account for their chamber by the correction factor k_{an} (axial non-uniformity of the beam). In order to investigate this effect the following beam geometries were chosen in the MC calculations:

1. Parallel beam, which is not subject to the inverse square law and produces a nearly constant photon fluence over the chamber region. The small deviation from constancy is only caused by the attenuation and scatter of the beam due to the chamber structure.
2. Divergent beam from a point source. This beam is subject to the inverse square law.

The ratio of the primary energies deposited in the cavity and corrected for attenuation and scatter for the parallel and divergent beam can be considered as the axial non-uniformity correction. All calculation runs, with typically $2*10^9$ primary photon histories each, resulted in ratios not significantly different from unity with a type A uncertainty of about 0.1 % for the ^{137}Cs as well as for the ^{60}Co beam. Therefore it must be concluded, that there is no axial non-uniformity effect to that extent, which could be expected from the considerations given above. The results are in agreement with those from other authors [3,6].

Experiments

The findings from the MC calculations concerning the axial non-uniformity correction are supported by the following experiments, which were conducted at our laboratory. For this purpose two experimental graphite cavity chambers were manufactured, which are different to our standard chamber CC01 with respect to size and volume. They are denoted as “Small” and “Large” in table1. The thickness of the chamber wall (4 mm) is the same for all three chambers. The two experimental chambers and the standard chamber CC01 were exposed at three different distances (50 cm, 100 cm and 200 cm) to the γ-radiation from our ^{60}Co teletherapy source.

If there were an axial non-uniformity effect subject to the inverse square law as discussed above, then this effect would result in a different response of the chambers at different distances and therefore would be detected in these measurements. Or in other words: If the effective point of measurement were not in the geometrical centre of the chamber, the ratio of the ionisation currents of the different chambers could be expected to be different at different distances. All ionisation currents were corrected for volume recombination. Possible differences for k_{at} and k_{sc} at the different irradiation distances were assumed to be not significant.

The results are given in table 4. They indicate, that there is no significant effect (at the confidence level due to a coverage factor k = 2) associated with the axial non-uniformity of the photon fluence from a divergent ^{60}Co beam. Therefore the effective point of measurement can be assumed to be in the geometrical centre of the chamber. This means that the energy deposited in the cavity is almost the same for a parallel and a divergent beam, although the electron production in the cylindrical chamber wall is higher in the case of the divergent beam (because of the inverse square law). Obviously, this higher production is compensated by the divergence of the electron cloud, which in average has the same density and deposits the same energy in the cavity in the case of a parallel and a divergent beam.

Conclusion

The correction factors for attenuation k_{at} and scatter k_{sc} were successfully calculated by the MC – code “PENELOPE” (version 2001). Calculations of the axial non-uniformity of a divergent beam resulted in a correction not significantly different from unity. These findings were supported by irradiation of three different chambers in three different distances. The results are in agreement with calculations obtained by other authors, who used a different code. Together with the experimental results this gives sufficient confidence, that the new correction factors obtained by MC are correct and can be applied to the air kerma standards of the BEV in the future.

Acknowledgement

The author is indebted to Mr. W. Tiefenböck, who performed the measurements for this work.

References

1. BIPM 1994: Comparison of the Standards of Air Kerma and of Absorbed Dose to Water of the BEV and the BIPM for ^{60}Co γ-rays. Rapport BIPM-94/7 (1994).
2. BIPM 1995: Comparison of the Standards of Air Kerma of the BEV and the BIPM for ^{137}Cs and ^{60}Co γ-rays. Rapport BIPM-95/5 (1995).
3. D.W.O. Rogers and J. Treurniet: Monte Carlo calculated wall and axial non-uniformity corrections for primary standards of air kerma. NRCC Report PIRS-663 (1999).
4. A.F. Bielajew and D.W.O. Rogers: Implications of new correction factors on primary air kerma standards in ^{60}Co beams. Phys. Med. Biol. 37 (1992), pp. 1283-1291.
5. D.W.O. Rogers and A.F. Bielajew: Wall attenuation and scatter corrections for ion chambers: measurements versus calculations. Phys. Med. Biol. 35 (1990), pp. 1065-1078.
6. L. Büermann, H.-M. Kramer and I. Csete (PTB and OMH): Results supporting calculated wall correction factors for cavity chambers, CCRI(I)/01-18, 10 p.
7. PENELOPE – A Code System for Monte Carlo Simulation of Electron and Photon Transport, Workshop Proceedings, Issy-les-Moulineaux, France, 5-7 November 2001, Nuclear Energy Agency, Organisation for Economic Co-operation and Development, 2, rue André-Pascal, 75775 Paris Cedex16, France.
8. M. Boutillon and M.-T. Niatel: A Study of a Graphite Cavity Chamber for Absolute Exposure Measurements of ^{60}Co Gamma Rays. Metrologia 9, 139-146 (1973).

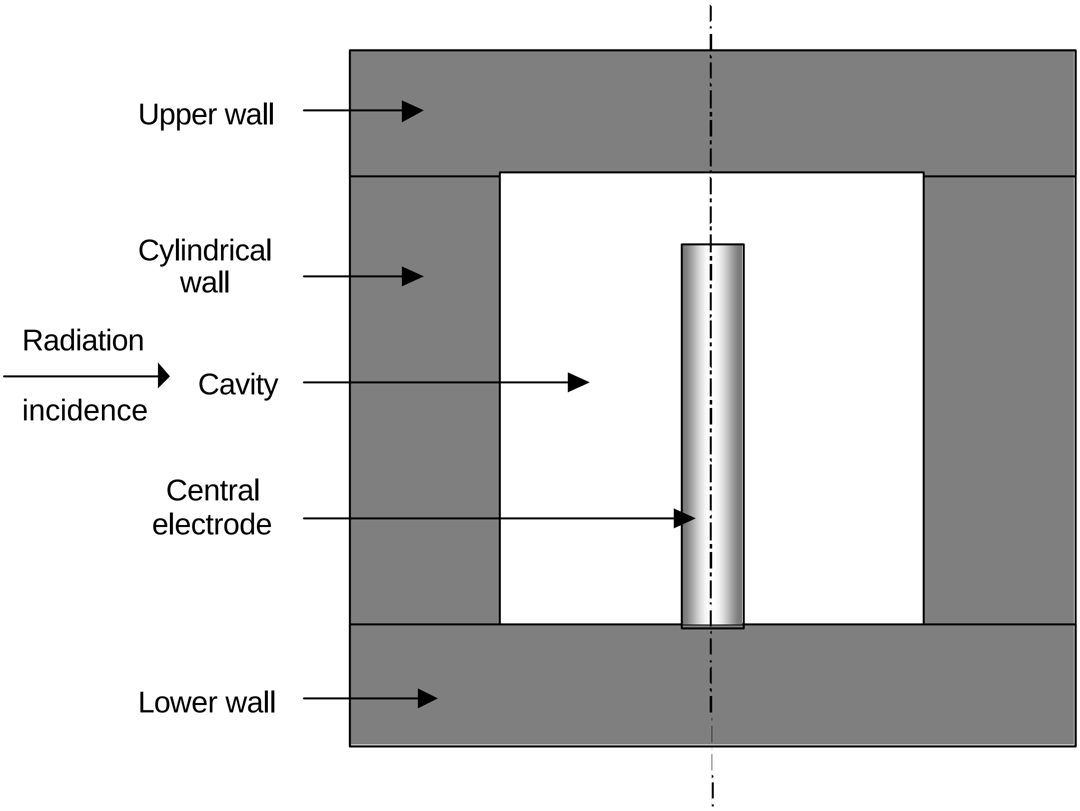

Figure 1: Simplified model of cylindrical graphite cavity chamber, type CC01, used in MC-calculation

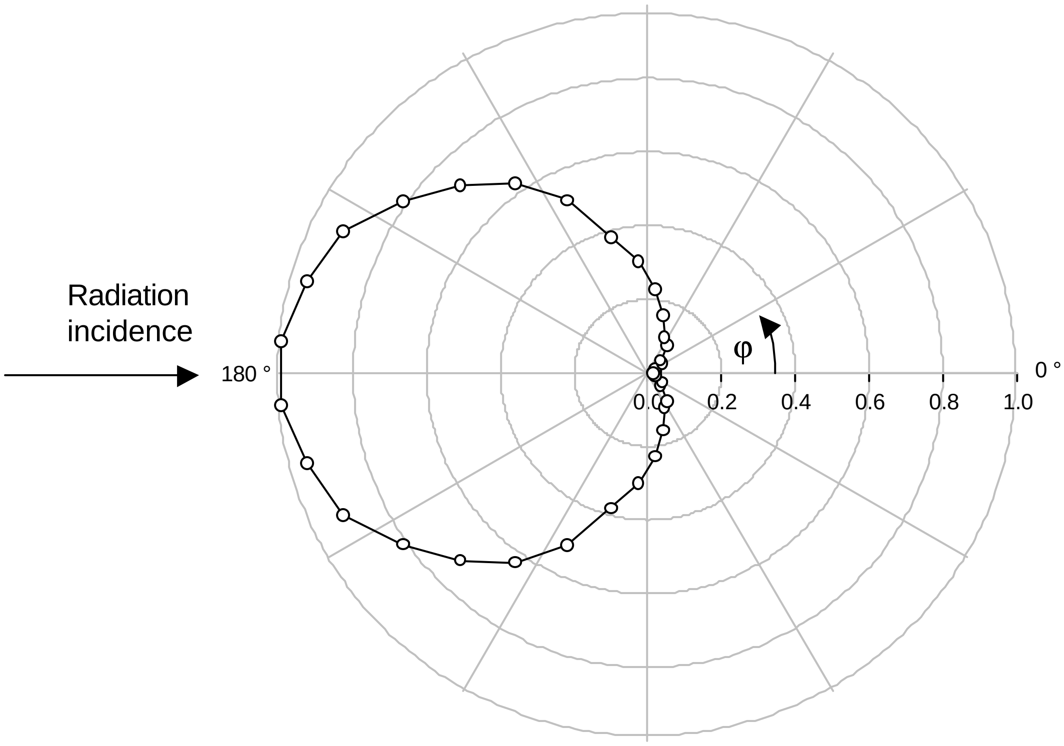

Diagram 1: Angular dependence of energy contribution $E(j)/E(180°)$ from cylindrical wall to primary energy deposited in cavity

Chamber type	**Small**	**CC01 (standard chamber at BEV)**	**Large**
Outer diameter	15 mm	19 mm	23 mm
Outer height	19 mm	19 mm	23 mm
Diameter of cavity	7 mm	11 mm	15 mm
Height of cavity	11 mm	11 mm	15 mm
Diameter of central electrode	2 mm	2 mm	2 mm
Height of central electrode	9 mm	9 mm	9 mm
Wall thickness	4 mm	4 mm	4 mm
Nominal volume	0.40 cm³	1.0 cm³	2.6 cm³

Table 1: Dimensions of cylindrical graphite cavity chambers, used for MC calculations and for axial non-uniformity experiments

^{137}Cs					
Chamber	**k_{at}(MC)**	**k_{sc}(MC)**	**$k_{at}*k_{sc}$(MC)**	**$k_{at}*k_{sc}*k_{cep}$(EX)**	**$k_{at}*k_{sc}$(MC)/ $k_{at}*k_{sc}*k_{cep}$(EX)**
CC01 SN 125	1.080 5	0.951 2	**1.027 8**	**1.017 1**	**1.010 5**
CC01 SN 132	1.084 5	0.948 9	**1.029 1**	**1.019 0**	**1.009 9**

^{60}Co					
Chamber	**k_{at}(MC)**	**k_{sc}(MC)**	**$k_{at}*k_{sc}$(MC)**	**$k_{at}*k_{sc}*k_{cep}$(EX)**	**$k_{at}*k_{sc}$(MC)/ $k_{at}*k_{sc}*k_{cep}$(EX)**
CC01 SN 125	1.055 3	0.967 3	**1.020 8**	**1.012 7**	**1.008 0**
CC01 SN 132	1.058 2	0.965 6	**1.021 8**	**-**	**-**

Table 2: Wall correction factors obtained by Monte Carlo (MC) and extrapolation (EX) – technique.

Body	**Relative contribution, %**
Lower wall	12.6
Central electrode	5.0
Cavity	0.5
Cylindrical wall	68.8
Upper wall	13.2

Table 3: Relative contribution from the different bodies to the primary energy deposited in the cavity.

Irradiation distance	**50 cm**			**100 cm**			**200 cm**		
Chamber	Small	CC01	Large	Small	CC01	Large	Small	CC01	Large
Ionisation current I, pA	497.94	1263.3	3228.5	112.86	285.99	730.36	27.606	69.975	178.65
I/I_{CC01}	0.3942	1	2.5557	0.3946	1	2.5538	0.3945	1	2.5531
$(I/I_{CC01})/(I/I_{CC01})_{100}$	**0.998 9**	**-**	**1.000 8**	**1**	**-**	**1**	**0.999 7**	**-**	**0.999 7**
Uncertainty, % (k=1)	0.06	-	0.06	-	-	-	0.06	-	0.06

Table 4: Experimental results of ionisation current measurements with three different ionisation chambers at three different distances.